The Journal of Chemical Physics

Communication: Contact values of pair distribution functions in colloidal hard disks by test-particle insertion

Cite as: J. Chem. Phys. **148**, 241102 (2018); https://doi.org/10.1063/1.5038668
Submitted: 04 May 2018 . Accepted: 06 June 2018 . Published Online: 28 June 2018

Adam Edward Stones, Roel P. A. Dullens, and Dirk G. A. L. Aarts

Communication: Contact values of pair distribution functions in colloidal hard disks by test-particle insertion

Adam Edward Stones,[a] Roel P. A. Dullens, and Dirk G. A. L. Aarts[b]
Physical and Theoretical Chemistry Laboratory, South Parks Road, Oxford OX1 3QZ, United Kingdom

(Received 4 May 2018; accepted 6 June 2018; published online 28 June 2018)

We apply Henderson's method for measuring the cavity distribution function $y(r)$ [J. Henderson, Mol. Phys. **48**, 389 (1983)] to obtain the pair distribution function at contact, $g(\sigma^+)$. In contrast to the conventional distance-histogram method, no approximate extrapolation to contact is required. The resulting equation of state from experiments and simulations of hard disks agrees well with the scaled particle theory prediction up to high fluid packing fractions. We also provide the first experimental measurement of $y(r)$ inside the hard core, which will allow for a more complete comparison with theory. The method's flexibility is further illustrated by measuring the partial pair distribution functions of binary hard-disk mixtures in simulation. The equation for the contact values can be used to derive familiar results from statistical geometry. *Published by AIP Publishing.* https://doi.org/10.1063/1.5038668

I. INTRODUCTION

The pair distribution function $g(r)$ is of central importance in the description of fluids: a real-space visualisation of the pairwise structure, its accurate determination also yields the structure factor, compressibility, pressure, and internal energy by integration.[1,2] Of particular interest is the value at contact in hard-particle systems, $g(\sigma^+)$, which is related to the pressure[1,2] and can be used to measure the equation of state and hence obtain a full thermodynamic description of the fluid. The contact value is also important in theories of transport processes in gases.[2,3] The conventional distance-histogram method for measuring $g(r)$ does not directly provide accurate results for the contact value, instead requiring an approximate extrapolation[4–11] since space is discretised into bins of finite width. Here we demonstrate an alternative approach for measuring $g(r)$ based on Henderson's method[12,13] for measuring the cavity distribution function $y(r)$. Use of this method in simulation has focussed on measuring bridge functions,[14–22] calculating Henry's law constants for dispheres,[23] and applying zero separation theorems;[24] here we show it can be used to measure $g(\sigma^+)$ without approximation in simulation and experiment.

We will begin by rederiving the key result of Henderson[12] for multi-component systems using a similar approach to Lee and Shing.[24] We will demonstrate its use in simulations and experiments of colloidal hard disks. We show that the measured contact values result in excellent agreement with the scaled particle theory equation of state[25,26] up to moderately high fluid densities. We illustrate the generality of the method by measuring the partial pair distribution functions in a binary hard-disk simulation. Finally we show that the expression for the contact values can be substituted into the pressure equation to straightforwardly derive familiar results from statistical geometry.[27,28]

[a]Electronic mail: adam.stones@chem.ox.ac.uk
[b]Electronic mail: dirk.aarts@chem.ox.ac.uk

II. THEORY

The potential distribution theorem in a multi-component inhomogeneous system is given by[13,29,30]

$$z_\alpha = \frac{\rho_\alpha(\mathbf{r})\exp(v_\alpha(\mathbf{r})/k_\mathrm{B}T)}{\langle\exp(-\Psi_\alpha/k_\mathrm{B}T)\rangle_\mathbf{r}}, \tag{1}$$

where $z_\alpha = \exp(\mu_\alpha/k_\mathrm{B}T)/\Lambda_\alpha^d$ is the reduced activity of a species α (μ_α is its chemical potential, Λ_α is its thermal wavelength, d is the dimensionality, and $k_\mathrm{B}T$ is the thermal energy), $\rho_\alpha(\mathbf{r})$ is the local number density at the position $\mathbf{r}$, and $v_\alpha(\mathbf{r})$ is a one-body external potential, which acts on α-particles. The quantity $\Psi_\alpha(\mathbf{r})$ in the denominator is the additional potential energy due to the hypothetical insertion of a test particle of α at $\mathbf{r}$, with the angled brackets denoting an average over the statistical ensemble. Note that z_α (and hence μ_α) is constant everywhere in an equilibrium inhomogeneous system, although here it is written as a ratio of spatially dependent quantities.[13]

Now consider a multi-component homogeneous system and describe the positions of all the other particles relative to an individual β-particle. Following this coordinate transformation, the homogeneous system can instead be described as an inhomogeneous system in which the other particles experience an external potential due to their pairwise interaction with the β-particle fixed at the origin, i.e., $v_\alpha(\mathbf{r}) = u_{\alpha\beta}(\mathbf{r})$. In this case, the number density in (1) is given by $\rho_\alpha^{(\beta)}(\mathbf{r}) = \rho_\alpha g_{\alpha\beta}(\mathbf{r})$, where $\rho_\alpha^{(\beta)}(\mathbf{r})$ is the number density of species α at $\mathbf{r}$ with a β-particle fixed at the origin and $g_{\alpha\beta}(\mathbf{r})$ is the pair distribution function between species α and β. Likewise, the ensemble average in (1) is given by $[\exp(-\Psi_\alpha/k_\mathrm{B}T)]_\mathbf{r}^{(\beta)}$, where $[\ldots]^{(\beta)}$ denotes an ensemble average in the inhomogeneous description with a β-particle fixed at the origin. Importantly, interactions of the test particle with the fixed particle are accounted for through the external potential and do not contribute to Ψ_α here. From (1), the activity of α is therefore given by

$$z_\alpha = \frac{\rho_\alpha g_{\alpha\beta}(\mathbf{r}) \exp(u_{\alpha\beta}(\mathbf{r})/k_\mathrm{B}T)}{[\exp(-\Psi_\alpha/k_\mathrm{B}T)]_\mathbf{r}^{(\beta)}}. \quad (2)$$

If instead the homogeneous system is considered without the transformation (i.e., $v = 0$ for all species), (1) reduces to

$$z_\alpha = \frac{\rho_\alpha}{\langle \exp(-\Psi_\alpha/k_\mathrm{B}T)\rangle}, \quad (3)$$

where, in addition to the activity, the density and ensemble average are also spatially independent.

Since μ_α (and hence z_α) is invariant under the coordinate transformation, (2) and (3) can be equated to yield

$$y_{\alpha\beta}(\mathbf{r}) = \frac{[\exp(-\Psi_\alpha/k_\mathrm{B}T)]_\mathbf{r}^{(\beta)}}{\langle \exp(-\Psi_\alpha/k_\mathrm{B}T)\rangle}, \quad (4)$$

where we have introduced the cavity distribution function

$$y_{\alpha\beta}(\mathbf{r}) = g_{\alpha\beta}(\mathbf{r}) \exp(u_{\alpha\beta}(\mathbf{r})/k_\mathrm{B}T), \quad (5)$$

which can be seen as the hypothetical pair distribution function between a pair of particles whose mutual interaction is zero, but whose interactions with all other particles remain the same.[2] In a fluid, $y_{\alpha\beta}(\mathbf{r})$ decays to 1 at large r, where the local and bulk averages in the numerator and the denominator in (4) are the same. Equation (4) is superficially similar to the more common definition of the pair distribution function as the ratio of the local number density around a reference particle and the bulk number density,

$$g_{\alpha\beta}(\mathbf{r}) = \frac{\rho_\alpha^{(\beta)}(\mathbf{r})}{\rho_\alpha}. \quad (6)$$

Equation (4) is general, but in this communication, we will deal only with hard disks, where the pairwise interaction $u_{\alpha\beta}(r)$ between species α and β is given by

$$u_{\alpha\beta}(r) = \begin{cases} 0 & \text{if } r > \sigma_{\alpha\beta}, \\ \infty & \text{if } r \le \sigma_{\alpha\beta}. \end{cases} \quad (7)$$

where r is the particles' separation and $\sigma_{\alpha\beta} = (\sigma_\alpha + \sigma_\beta)/2$ is the separation of an α-particle and a β-particle in contact. The Boltzmann factor in the denominator of (4) is zero when the test particle overlaps with a particle of the system and unity otherwise, and the ensemble average reduces to the insertion probability[2] of an α-particle in the homogeneous system, P_ins^α. Likewise, the numerator is given by $P_\mathrm{ins}^{\alpha(\beta)}(\mathbf{r})$, i.e., the probability of inserting an α-particle at $\mathbf{r}$ given that there is a β-particle fixed at the origin. The cavity distribution function is then given by

$$y_{\alpha\beta}(\mathbf{r}) = \frac{P_\mathrm{ins}^{\alpha(\beta)}(\mathbf{r})}{P_\mathrm{ins}^\alpha}, \quad (8)$$

i.e., as a ratio of local and bulk insertion probabilities. For hard disks, $g_{\alpha\beta}$ is identical to $y_{\alpha\beta}$ except inside the core ($r < \sigma_{\alpha\beta}$), where $g_{\alpha\beta}(\mathbf{r}) = 0$, as follows from (5). Note that while both $g_{\alpha\beta}$ and $u_{\alpha\beta}$ have a discontinuity at $r = \sigma_{\alpha\beta}$, $y_{\alpha\beta}$ is continuous[2] for all r.

While both (4) and (6) are theoretically sound, if the pair potential $u_{\alpha\beta}$ is known, (4) can be more useful in measurements of $g_{\alpha\beta}$ from simulation and experimental real-space coordinate data. The local density $\rho_\alpha^{(\beta)}(\mathbf{r})$ in (6) requires division by an infinitesimal volume element and is therefore not amenable to direct practical calculation, instead requiring the volume elements to be replaced by small but finite volumes as employed in the conventional distance-histogram method.[4] The measured $g_{\alpha\beta}$ is therefore the convolution of the *true* $g_{\alpha\beta}$ with a boxcar function depending on the size of these volumes,[11] and the sharp peak expected for hard particles is obscured. The chosen volume sizes are a compromise: larger volumes result in reduced statistical noise but greater smoothing by the convolution and hence greater loss of structural information. In low-density systems, very long experiments and simulations may be required to achieve acceptable statistics.

By contrast, the test-particle insertion approach based on (4) avoids the finite-volume problem altogether since insertions are attempted at precise separations from a central particle, and so $g_{\alpha\beta}(\sigma_{\alpha\beta}^+)$ can be measured directly, without extrapolation. Furthermore, the cavity distribution function $y_{\alpha\beta}$ can be measured at all separations, including those inside the hard core which are inaccessible using the density approach. The method is particularly useful at low densities, where accurate determination of the insertion probabilities is straightforward—in this sense, it is complementary to the distance-histogram method, which is more effective at higher densities due to better statistics.

Once $g_{\alpha\beta}$ is known, there are several routes to the thermodynamics of the fluid[1,2]—the isothermal compressibility can be calculated by integration, as can the internal energy and pressure if the pair potential is known. For hard particles, the integral in the pressure equation can be performed analytically, yielding an equation of state which depends only on values of the pair distribution functions at contact.[1,2] For multi-component hard-disk mixtures,[31]

$$\frac{P}{k_\mathrm{B}T} = \sum_\alpha \rho_\alpha + \frac{\pi}{2} \sum_{\alpha\beta} \rho_\alpha \rho_\beta \sigma_{\alpha\beta}^2 g_{\alpha\beta}(\sigma_{\alpha\beta}^+), \quad (9)$$

where P is the pressure and the sums run over all components of the system. For single-component hard disks, (9) reduces to

$$\frac{P}{\rho k_\mathrm{B}T} = 1 + 2\phi g(\sigma^+), \quad (10)$$

where the packing fraction $\phi = \rho\pi\sigma^2/4$.

III. METHODS

A. Experiments

Carboxylic acid-functionalised melamine formaldehyde (MF) spheres (Microparticles GmbH) in 20%/80% v/v ethanol/water were allowed to sediment in a quartz glass cell (Hellma Analytics) to form a quasi-two-dimensional colloidal monolayer, which has been shown to behave structurally as a hard-disk model system with diameter $\sigma = 2.79\ \mu$m.[11,32] Samples of different packing fractions were imaged every second for 30 min using an Olympus CKX41 bright-field microscope fitted with a 40× objective and a Ximea XIQ CMOS camera. The particle locations were found using standard routines.[33,34]

B. Simulations

For the single-component simulations, we used the event-chain Monte Carlo algorithm of Bernard *et al.*,[35] which allows for an independent measure of the pressure using the simulation dynamics.[36] A fixed number of disks (1024) were equilibrated and the box size was adjusted to achieve the desired volume fraction. For the binary simulation, we used the local Metropolis algorithm[37] to equilibrate an equal number of disks with a size ratio $\sigma_l/\sigma_s = 4/3$ in a box of length $50\sigma_l$. In both cases, periodic boundary conditions were employed to reduce finite-size effects.

C. Insertion probabilities

We determined the local insertion probability $P_{\text{ins}}^{\alpha(\beta)}(\mathbf{r})$ by trial insertion on a grid around each particle, for each analyzed frame. For the experiments, insertions were attempted at 10 different angles at radial distances from 0 to 10σ (separated by 0.05σ). In contrast to the distance-histogram method, the measurement at each distance is independent, and so smaller separations could be used without an increase in statistical noise. In the single-component simulation, a radial separation of 0.1σ was used and 5000 frames were analyzed. In the binary simulation, 10 000 frames were analyzed, with 20 angles and radial distances separated by $0.1\sigma_{\alpha\beta}$, depending on the identities of the test particle and the particle about which insertions were attempted. A separate measurement of the bulk insertion probability was performed in each case by attempting particle insertions on a grid over the field of view or simulation box.

IV. RESULTS AND DISCUSSION

Figure 1(a) shows the $g(r)$ measured in a simulation of packing fraction $\phi = 0.35$ using both the insertion method and the distance-histogram method. Two different sets of bin locations were used with a bin width of 0.1σ—for both locations, the behavior of $g(r)$ at contact is not captured correctly (see the inset). In the case where the contact radius coincides with a bin centre, the measured contact value is significantly underestimated since the bin partially overlaps with the core ($r < \sigma$), where there are strictly no other particles due to the hard-disk pair potential (7). In the second case, the contact radius coincides with a bin edge, and although the corresponding bin (to the right of contact) yields a value which agrees well with that of the insertion method, the mid-point of the bin is not at the contact radius and an approximate extrapolation is required to calculate the contact value.[4] By contrast, the method based on insertion allows measurement of $g(\sigma^+)$ without approximation—the measured value shows good agreement with the prediction of scaled particle theory (dashed line), which is known to work well at this packing fraction.[11] Note that away from the contact region, the three analyses give essentially identical results: the effect of the convolution is considerably less pronounced in regions where $g(r)$ is slowly varying.

Figure 1(b) shows experimental measurements of $g(r)$ at three packing fractions. Again, the discontinuity at contact is well-captured by construction, and the structure of the fluid has the damped oscillatory decay expected at such packing fractions. The inset shows the corresponding $y(r)$ measurements including those inside the core (note that outside the core, $g(r) = y(r)$ for hard disks). While $y(r)$ inside the core has been measured in simulations (using Henderson's method[16] or an alternative[38]), this first experimental measurement opens the possibility of assessing the reliability of both experimental model systems and theories.[39,40] Furthermore, $y(r)$ is linked directly to thermodynamics via zero separation theories,[24,41,42] and $y(r)$ for hard particles plays a central role in certain perturbation theories.[38,43,44]

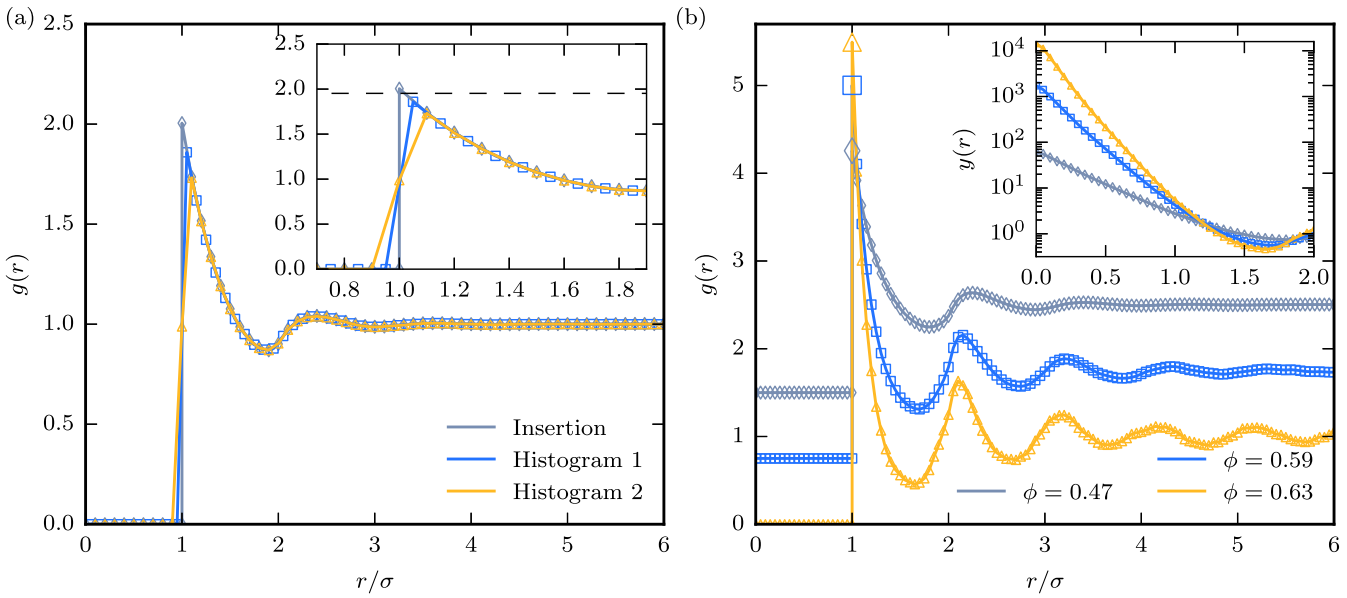

FIG. 1. (a) Comparison of the $g(r)$ obtained in *simulation* ($\phi = 0.35$) by insertion (diamonds) and the distance-histogram method with two different bin locations (squares, triangles). Inset: zoom of the contact region; the dashed line is the scaled particle theory prediction of the contact value. (b) $g(r)$ measured using insertion in *experiment* at three different packing fractions; for clarity, the results for $\phi = 0.59$ and $\phi = 0.47$ have been shifted by 0.75 and 1.50, respectively, and the contact values are displayed with larger symbols. Inset: corresponding $y(r)$ on a semi-log plot.

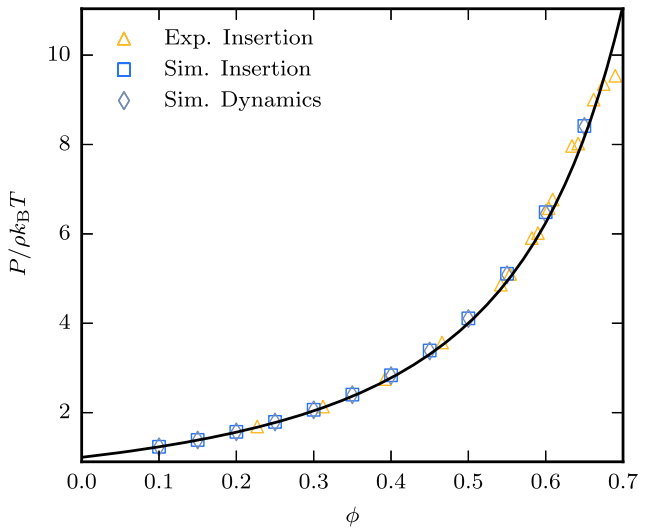

FIG. 2. Compressibility factor $Z = P/\rho k_B T$ calculated using the single-component contact values $g(\sigma)$ measured in experiment and simulation. For comparison, the values from the simulation dynamics are shown, as is the scaled particle theory equation of state (black line).

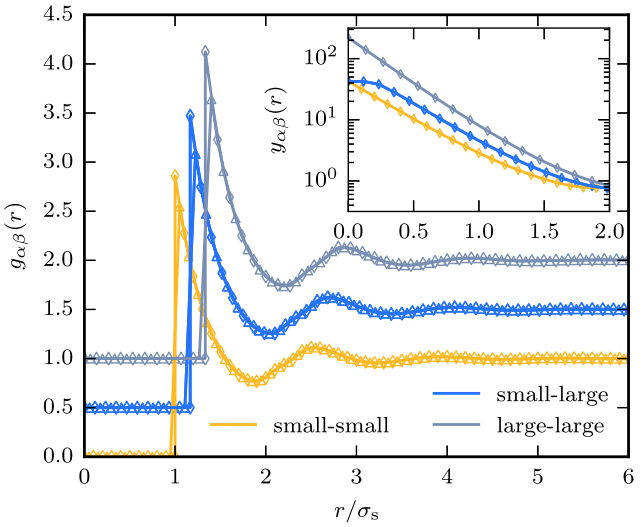

FIG. 3. Binary hard-disk partial pair distribution functions $g_{ss}(r)$, $g_{sl}(r) = g_{ls}(r)$, and $g_{ll}(r)$ measured by insertion (diamonds) and the distance-histogram method (triangles) in simulation. The total packing fraction $\phi_{total} = 0.49$, with an equal number of large and small disks with size ratio $\sigma_l/\sigma_s = 4/3$. For clarity, $g_{sl}(r)$ and $g_{ll}(r)$ have been shifted by 0.5 and 1.0, respectively. Inset: the corresponding partial cavity distribution functions on a semi-log plot.

The contact values are then used in (10) to calculate the compressibility factor $Z = P/\rho k_B T$ and hence the pressure equation of state, shown in Fig. 2. The results from simulation and experiments agree well with the scaled particle theory prediction up to high fluid packing fractions (Thorneywork *et al.* found the fluid-hexatic coexistence region to be at $\phi \approx 0.68$–0.70 in the same system[32]). Furthermore, the event-chain simulation dynamics allow for an independent route to the pressure,[36] with which excellent agreement is found. This further demonstrates the validity of this system as an experimental model for hard disks, as previously shown by Thorneywork *et al.*[11,32] where the contact value was found by extrapolation.

The generality of the method is further illustrated by calculating the partial pair distribution functions in the binary hard-disk simulation, which are again compared with the distance-histogram results in Fig. 3. The corresponding partial cavity distribution functions are shown in the inset and display some noteworthy features which can be understood using (8).[45] The coincidence of y_{ss} and $y_{sl} = y_{ls}$ at $r = 0$ is understood by noting that $P_{ins}^{s(s)}(0) = P_{ins}^{s(l)}(0) = 1$, since in both cases the fixed particle prevents other particles from overlapping with the region where the test particle is inserted. From (8), it follows that $y_{ss}(0) = y_{sl}(0) = 1/P_{ins}^{s}$. Moreover, since in the case of a large fixed particle, $P_{ins}^{s(l)}(r) = 1$ for $0 < r < (\sigma_l - \sigma_s)/2$, the value of y_{sl} is constant for these values of r. Note that while $P_{ins}^{l(s)}(r) < 1$ over this range, the equality $y_{sl} = y_{ls}$ is maintained since the bulk insertion probability for large particles is less than that for small particles (i.e., $P_{ins}^{l} < P_{ins}^{s}$).

In contrast to the distance-histogram method, the equality $g_{sl}(r) = g_{ls}(r)$ predicted by statistical mechanics is not strictly enforced by the insertion method, where these two functions are measured separately by considering the insertion of large particles about small particles and vice versa according to (8). Although numerically minor differences are observed due to noise, both functions are plotted in Fig. 3 where their difference is not distinguishable. The convergence of these functions may be used to test whether enough data have been acquired to provide reliable statistics. A direct link to the thermodynamics of the binary fluid is provided by (9), which in conjunction with the method presented here will allow for a more complete study of the thermodynamics of hard-disk mixtures. Finally, we note that the method is readily extended to fluids with more than two components and of higher dimensionality.

V. LINK WITH STATISTICAL GEOMETRY

Finally, the expression (8) for the cavity distribution function at contact ($r = \sigma_{\alpha\beta}$) allows for an elegant link between the thermodynamics of hard disks and certain geometric quantities: in the single-component case, these are the average volume available for test-particle insertion, V_s, and the surface area of this volume, A_s.[27] Similar results have been derived for multi-component systems[28] and can be derived very quickly here (in a similar spirit to Speedy's original derivation for the single-component case[27]) by substituting (8) into (9) after noting that $g_{\alpha\beta}(\sigma_{\alpha\beta}^{+}) = y_{\alpha\beta}(\sigma_{\alpha\beta})$ for hard systems to yield

$$\frac{P}{k_B T} = \sum_i \rho_i + \frac{\pi}{2} \sum_{\alpha,\beta} \rho_\alpha \rho_\beta \sigma_{\alpha\beta}^2 \frac{P_{ins}^{\alpha(\beta)}(\sigma_{\alpha\beta})}{P_{ins}^{\alpha}}. \tag{11}$$

The insertion probabilities are related to geometric quantities by first noting that $P_{ins}^{\alpha} = \langle V_s^{\alpha} \rangle / V$, where $\langle V_s^{\alpha} \rangle$ is the average volume available for the insertion of a test particle of species α. The local insertion probability $P_{ins}^{\alpha(\beta)}(\sigma_{\alpha\beta}) = \langle A_s^{\alpha(\beta)} \rangle / 2\pi\sigma_{\alpha\beta} N_\beta$, where $\langle A_s^{\alpha(\beta)} \rangle$ is the component of the surface area of the volume available for α-particle insertion which is due to contact with β-particles and N_β is the total

number of β-particles. This ratio is the average fraction of the circle of radius $\sigma_{\alpha\beta}$ around each β-particle which is available for α-particle insertion. Substituting these into (11) gives

$$\frac{P}{k_{\mathrm{B}}T} = \sum_{\alpha} \rho_{\alpha} + \frac{1}{4} \sum_{\alpha\beta} \rho_{\alpha}\sigma_{\alpha\beta} \frac{\langle A_{\mathrm{s}}^{\alpha(\beta)} \rangle}{\langle V_{\mathrm{s}}^{\alpha} \rangle}, \tag{12}$$

which is the 2D version of the result derived by Corti and Bowles.[28] The result (12) extends straightforwardly to fluids in higher dimensions[27,28] and has indeed been used in experiments on colloidal hard spheres.[46]

VI. CONCLUSION

We have applied Henderson's method[12] to measure the cavity distribution function in colloidal experiments and simulations, which we subsequently used to obtain the contact values of pair distribution functions in single- and multi-component hard-disk fluids. In the single-component case, the measured equation of state agrees well with scaled particle theory. We have measured the cavity correlation function inside the core for the first time experimentally, which will allow further comparisons between theory and experiment. Finally we have shown that this result for the contact value allows straightforward derivation of statistical geometrical results for hard particles. The results can be readily extended to higher dimensions and will allow for a more complete thermodynamic study of hard-sphere mixtures. In principle, these methods can be extended to investigate many-body distribution functions and more complex fluids, such as those composed of hard rods or molecules composed of fused hard spheres.[4]

ACKNOWLEDGMENTS

A.E.S. gratefully acknowledges financial support from the University of Oxford Clarendon Fund. Bob Evans, Alice Thorneywork, and Andrew Parry are thanked for useful discussions.

[1] J. A. Barker and D. Henderson, Rev. Mod. Phys. **48**, 587 (1976).
[2] J.-P. Hansen and I. McDonald, *Theory of Simple Liquids: With Applications to Soft Matter*, 4th ed. (Academic Press, 2013).
[3] M. López de Haro, E. G. D. Cohen, and J. M. Kincaid, J. Chem. Phys. **78**, 2746 (1983).
[4] M. P. Allen and D. J. Tildesley, *Computer Simulation of Liquids* (Oxford Science Publications, Clarendon Press, 1989).
[5] B. Freasier, Mol. Phys. **39**, 1273 (1980).
[6] J. Tobochnik and P. M. Chapin, J. Chem. Phys. **88**, 5824 (1988).
[7] M. Barošová, M. Malijevský, S. Labík, and W. Smith, Mol. Phys. **87**, 423 (1996).
[8] D. Cao, K. Chan, D. Henderson, and W. Wang, Mol. Phys. **98**, 619 (2000).
[9] M. González-Melchor, J. Alejandre, and M. López de Haro, J. Chem. Phys. **114**, 4905 (2001).
[10] E. P. Bernard and W. Krauth, Phys. Rev. Lett. **107**, 155704 (2011).
[11] A. L. Thorneywork, R. Roth, D. G. A. L. Aarts, and R. P. A. Dullens, J. Chem. Phys. **140**, 161106 (2014).
[12] J. Henderson, Mol. Phys. **48**, 389 (1983).
[13] B. Widom, J. Stat. Phys. **19**, 563 (1978).
[14] M. Llano-Restrepo and W. G. Chapman, J. Chem. Phys. **97**, 2046 (1992).
[15] M. Llano-Restrepo and W. G. Chapman, J. Chem. Phys. **100**, 5139 (1994).
[16] R. Fantoni and G. Pastore, J. Chem. Phys. **120**, 10681 (2004).
[17] D. L. Cheung, L. Anton, M. P. Allen, and A. J. Masters, Phys. Rev. E **73**, 061204 (2006).
[18] T. R. Kunor and S. Taraphder, Phys. Rev. E **74**, 011201 (2006).
[19] D. L. Cheung, L. Anton, M. P. Allen, and A. J. Masters, Comput. Phys. Commun. **179**, 61 (2008).
[20] J. Puibasset and L. Belloni, J. Chem. Phys. **136**, 154503 (2012).
[21] A. R. Saeger, J. K. Johnson, W. G. Chapman, and D. Henderson, Mol. Phys. **114**, 2516 (2016).
[22] J. K. Johnson, D. Henderson, S. Labík, and A. Malijevský, Mol. Phys. **115**, 1335 (2017).
[23] D. Ghonasgi, M. Llano-Restrepo, and W. G. Chapman, J. Chem. Phys. **98**, 5662 (1993).
[24] L. L. Lee and K. S. Shing, J. Chem. Phys. **91**, 477 (1989).
[25] H. Reiss, H. L. Frisch, and J. L. Lebowitz, J. Chem. Phys. **31**, 369 (1959).
[26] E. Helfand, H. L. Frisch, and J. L. Lebowitz, J. Chem. Phys. **34**, 1037 (1961).
[27] R. J. Speedy, J. Chem. Soc., Faraday Trans. 2 **76**, 693 (1980).
[28] D. S. Corti and R. K. Bowles, Mol. Phys. **96**, 1623 (1999).
[29] B. Widom, J. Chem. Phys. **39**, 2808 (1963).
[30] J. Henderson, Mol. Phys. **50**, 741 (1983).
[31] A. Santos, S. B. Yuste, and M. L. de Haro, J. Chem. Phys. **117**, 5785 (2002).
[32] A. L. Thorneywork, J. L. Abbott, D. G. A. L. Aarts, and R. P. A. Dullens, Phys. Rev. Lett. **118**, 158001 (2017).
[33] J. C. Crocker and D. G. Grier, J. Colloid Interface Sci. **179**, 298 (1996).
[34] D. Allan, T. Caswell, N. Keim, and C. van der Wel, trackpy: Trackpy v0.3.0, 2015.
[35] E. P. Bernard, W. Krauth, and D. B. Wilson, Phys. Rev. E **80**, 056704 (2009).
[36] M. Michel, S. C. Kapfer, and W. Krauth, J. Chem. Phys. **140**, 054116 (2014).
[37] N. Metropolis, A. W. Rosenbluth, M. N. Rosenbluth, A. H. Teller, and E. Teller, J. Chem. Phys. **21**, 1087 (1953).
[38] G. Torrie and G. Patey, Mol. Phys. **34**, 1623 (1977).
[39] G. Brenan and R. Evans, Mol. Phys. **73**, 789 (1991).
[40] R. Roth, K. Mecke, and M. Oettel, J. Chem. Phys. **136**, 081101 (2012).
[41] W. G. Hoover and J. C. Poirier, J. Chem. Phys. **37**, 1041 (1962).
[42] E. Meeron and A. J. F. Siegert, J. Chem. Phys. **48**, 3139 (1968).
[43] J. D. Weeks, D. Chandler, and H. C. Andersen, J. Chem. Phys. **55**, 5422 (1971).
[44] H. C. Andersen, J. D. Weeks, and D. Chandler, Phys. Rev. A **4**, 1597 (1971).
[45] E. Grundke and D. Henderson, Mol. Phys. **24**, 269 (1972).
[46] R. P. A. Dullens, D. G. A. L. Aarts, and W. K. Kegel, Proc. Natl. Acad. Sci. U. S. A. **103**, 529 (2006).